Cellular/Molecular

The $\alpha_2\delta$ Ligand Gabapentin Inhibits the Rab11-Dependent Recycling of the Calcium Channel Subunit $\alpha_2\delta$-2

Alexandra Tran-Van-Minh and Annette C. Dolphin
Department of Neuroscience, Physiology and Pharmacology, University College London, London WC1E 6BT, United Kingdom

The $\alpha_2\delta$ subunits of voltage-gated calcium channels are important modulatory subunits that enhance calcium currents and may also have other roles in synaptogenesis. The antiepileptic and antiallodynic drug gabapentin (GBP) binds to the $\alpha_2\delta$-1 and $\alpha_2\delta$-2 isoforms of this protein, and its binding may disrupt the binding of an endogenous ligand, required for their correct function. We have shown previously that GBP produces a chronic inhibitory effect on calcium currents by causing a reduction in the total number of $\alpha_2\delta$ and α_1 subunits at the cell surface. This action of GBP is likely to be attributable to a disruption of the trafficking of $\alpha_2\delta$ subunits, either to or from the plasma membrane. We studied the effect of GBP on the internalization of, and insertion into the plasma membrane of $\alpha_2\delta$-2 using an α-bungarotoxin binding site-tagged $\alpha_2\delta$-2 subunit, and a fluorescent derivative of α-bungarotoxin. We found that GBP specifically disrupts the insertion of $\alpha_2\delta$-2 from post-Golgi compartments to the plasma membrane, and this effect was prevented by a mutation of $\alpha_2\delta$-2 that abolishes its binding to GBP. The coexpression of the GDP-bound Rab11 S25N mutant prevented the GBP-induced decrease in $\alpha_2\delta$-2 cell surface levels, both in cell lines and in primary neurons, and the GBP-induced reduction in calcium channel currents. In contrast, the internalization of $\alpha_2\delta$-2 was unaffected by GBP. We conclude that GBP acts by preventing the recycling of $\alpha_2\delta$-2 from Rab11-positive recycling endosomes to the plasma membrane.

Introduction

Voltage-gated calcium channels (VGCCs) form a major route of entry for Ca^{2+} in excitable cells, where changes in Ca^{2+} concentration are crucial for many physiological processes. VGCCs of the Ca_v1 and Ca_v2 families are heteromeric complexes, made up of a pore-forming α_1 subunit, a cytosolic β subunit, and a membrane-anchored extracellular $\alpha_2\delta$ subunit (Catterall, 2000; Arikkath and Campbell, 2003; Davies et al., 2007, 2010). The coexpression of $\alpha_2\delta$ with α_1 and β subunits causes a threefold increase in calcium currents (Klugbauer et al., 1999; Canti et al., 2005), thought to be attributable to a trafficking mechanism to increase the number of VGCC complexes present at the plasma membrane (Canti et al., 2005; Bernstein and Jones, 2007).

The $\alpha_2\delta$-1 and -2 subunits are the pharmacological target of the antiepileptic and antiallodynic drugs gabapentin (GBP) and pregabalin (PGB). GBP was first designed as a GABA analog but has since been shown to have no effect on GABA systems (Lanneau et al., 2001; Jensen et al., 2002; Cheng et al., 2004). Instead, the binding of GBP and PGB to $\alpha_2\delta$-1 has been shown to be essential for their therapeutic effect (Field et al., 2006). Both drugs bind to an extracellular epitope present on the $\alpha_2\delta$-1 and -2 subunits (Brown et al., 1998), and their binding may disrupt the function of an unknown endogenous ligand (Hendrich et al., 2008). The mechanism of action of these drugs is controversial, with suggested mechanisms including acute inhibition of calcium currents (Sutton et al., 2002), chronic inhibition of calcium channel trafficking (Hendrich et al., 2008), and interference with $\alpha_2\delta$-1 binding to thrombospondin (Eroglu et al., 2009). In this study, we concentrated on the effect of GBP on $\alpha_2\delta$-2 because the disruption of the expression of $\alpha_2\delta$-2 causes an epileptic phenotype (Barclay et al., 2001; Ivanov et al., 2004). Several studies found that GBP has little or no acute effect on calcium currents or neurotransmitter release (Fehrenbacher et al., 2003; Brown and Randall, 2005). Recently, we reported that chronic, but not acute application of GBP causes a significant decrease in Ca^{2+} currents, only when the channels contain either $\alpha_2\delta$-1 or $\alpha_2\delta$-2 (Hendrich et al., 2008). This effect occurs intracellularly, as it requires GBP to be taken up by system-L transporters. In an *in vivo* study, we also showed that, during neuropathic pain, a condition in which the levels of $\alpha_2\delta$-1 subunit are upregulated in dorsal root ganglion neurons, the antiallodynic response to PGB is accompanied by an impairment of the anterograde trafficking of $\alpha_2\delta$-1 to presynaptic terminals (Bauer et al., 2009).

The mode of action whereby GBP inhibits the trafficking of $\alpha_2\delta$ subunits remains unknown. To address this question, we used an $\alpha_2\delta$-2 construct into which a 13 aa α-bungarotoxin (αBgTx) binding site (bbs) epitope was incorporated at an extracellular location, in conjunction with fluorescent derivatives of αBgTx. Using this method, we have now shown that GBP reduces the number of $\alpha_2\delta$-2 subunits present at the cell surface by preventing the Rab11-dependent recycling of these subunits to the plasma membrane.

Received May 27, 2010; revised July 29, 2010; accepted Aug. 5, 2010.

The work was supported by Medical Research Council Grant G0700368. A.T.-V.-M. was supported in part by a University College London Graduate Scholarship. We thank Dr. Terry Hébert (McGill University, Montreal, Quebec, Canada) for the Rab11 constructs, Prof. Mary McCaffrey (University College Cork, Cork, Ireland) for Rab4 constructs, Dr. Claudia Bauer for comments on this manuscript, and Kanchan Chaggar for technical support.

Correspondence should be addressed to either Alexandra Tran-Van-Minh or Annette C. Dolphin, Department of Neuroscience, Physiology and Pharmacology, University College London, Gower Street, London WC1E 6BT, UK, E-mail: a.tran-van-minh@ucl.ac.uk or a.dolphin@ucl.ac.uk.

DOI:10.1523/JNEUROSCI.2700-10.2010

 0270-6474/10/3012856-12$15.00/0

Materials and Methods

DNA constructs and expression. The sequence encoding the bbs epitope (WRYYESSLEPYPD) was introduced into the $\alpha_2\delta$-2 (GenBank accession number AF247139) sequence by PCR, at a position corresponding to the D589/E590 amino acids of $\alpha_2\delta$-2. Two bbs-containing fragments were generated using the primers 5′-TGGAGATACTACGAGAGCTCC-CTGGAGCCCTACCCTGACGAGAACAAGGAGGAGATC-3′ (sense) with 5′-CCGGAGTCACTTTCTCCATGAGCTCGATG-3′ (antisense), and 5′-CGATGTGGCCTTGAATGACATCAAAAGGC-3′ (sense) with 5′-GTCAGGGTAGGGCTCCAGGGAGCTCTCGTAGTATCTCCAAT-CTTCCAGCTCTGCGTC-3′ (antisense). Both fragments were reamplified together and phosphorylated, and then inserted into the $\alpha_2\delta$-2 sequence using the ClaI and AccIII restriction sites.

The sequence of $\alpha_2\delta$-2 containing the bbs epitope was subcloned from pMT2LF $\alpha_2\delta$-2 bbs into pMT2LF $\alpha_2\delta$-2 R282A using the endonucleases ClaI and BspEI.

Other cDNAs used were $\alpha_2\delta$-2 [hemagglutinin (HA)] (Davies et al., 2006), rat $Ca_v2.1$ (M64373), rat $\beta4$ (LO2315), all subcloned in pMT2, human Rab11-myc (AF000231) and Rab11 S25N-myc in pCMV (Dupré et al., 2006), and human Rab4 and Rab4 S22N in pEGFP (McCaffrey et al., 2001), and the chimeric nAChR α7-V201-5HT3A (Cooper and Millar, 1998).

For expression in cultured neurons, $\alpha_2\delta$-2 bbs was subcloned from pMT2LF into pcDNA 3.1 Zeo(+) (Invitrogen) using the endonucleases KpnI and NotI. pcDNA3.1 Zeo(+) eGFP-Rab11 wild-type (WT) and S25N were made by subcloning enhanced green fluorescent protein (eGFP) from pEGFP-C1 (Clontech) into pcDNA 3.1 Zeo(+) using the endonucleases NheI and BamHI, and then subcloning Rab11 WT or S25N from pCMV into the resulting plasmid using the endonucleases BamHI and NotI.

Antibodies. Primary antibodies used were as follows: affinity-purified rabbit anti-peptide anti-α_2-2 (Brodbeck et al., 2002) used at 1:1000, monoclonal rat anti-HA (Roche) used at 1:250, rabbit anti-green fluorescent protein (GFP) (Invitrogen) used at 1:500, and chicken anti-MAP2 (Abcam) used at 1:1000. All conjugated secondary antibodies were purchased from Invitrogen and used at a dilution of 1:1000.

Cell culture and transfection. tsA-201 cells were grown in DMEM (Invitrogen) supplemented with 10% fetal bovine serum, 100 U/ml penicillin and 100 U/ml streptomycin, and 2 mM GlutaMAX (Invitrogen). The cells were transfected using the FuGene reagent (Roche), following the manufacturer's instructions. In all experiments, the ratio of DNA/FuGene used was 2:3. Calcium channel subunits were transfected in a 3:2:2 ratio corresponding to $Ca_v2.1/\alpha_2\delta$-2/$\beta4$. In experiments with Rab proteins, the cDNA ratio was 3:2:2:2 for $Ca_v2.1/\alpha_2\delta$-2/$\beta4$/Rab4 or Rab11. Experiments were performed 2 d after transfection.

Immunocytochemistry. Cells were plated on glass coverslips coated with 15 mg/ml poly-L-lysine to ensure good adhesion of the cells and transfected. The cells were grown at 37°C for 48–72 h, and then washed twice in TBS and fixed with 3% paraformaldehyde in PBS for 5 min. Cells were then incubated for at least 1 h in a blocking solution consisting of 20% goat serum and 4% BSA in TBS, to reduce nonspecific binding of the antibodies. The primary antibodies were diluted in a 10% goat serum/2% BSA solution and applied overnight at 4°C. The coverslips were then washed four times with the blocking solution, before application of the secondary antibodies, for 2 h at room temperature. In some experiments, the nuclei were stained using 4′,6-diamidino-2-phenylindole (DAPI). The cells were then rinsed in TBS and mounted in Vectashield (Vector Laboratories) to reduce photobleaching.

For immunocytochemical experiments performed on neuronal cultures, plasma membrane-expressed proteins were immunodetected by live labeling with a primary antibody directed against an extracellular epitope, for 2 h at 37°C. Neurons were subsequently washed with PBS, and fixed for 10 min with a solution of 4% paraformaldehyde–4% sucrose in PBS. Permeabilization of the cells was then performed with PBS–0.1% Triton X-100 for 15 min. The cells were then incubated with a blocking solution consisting of 20% goat serum and 4% BSA in PBS, and incubated with primary antibodies directed against intracellular epitopes overnight at 4°C. Incubation with the appropriate secondary antibodies was performed for 2 h at room temperature. The imaging was performed using a confocal laser-scanning microscope (Zeiss) and a 63× [numerical aperture (NA), 1.4] oil-immersion objective. For experiments performed in neurons, optical sections of 1.2 μm thickness were acquired for each channel. The cell surface expression of $\alpha_2\delta$-2 in neurites was quantified by positioning regions of interest of similar size to those described in Figure 8*B*, 200–300 μm from the cell body and measuring the fluorescence density of these selections. The regions of interest pictured in Figure 8*B* were straightened using the ImageJ "Straighten" plug-in (Kocsis et al., 1991).

Electrophysiology. Calcium channel expression in tsA-201 cells was investigated by whole-cell patch-clamp recording. The internal (pipette) and external solutions and recording techniques were similar to those described previously (Brickley et al., 1995). The patch pipette solution contained the following (in mM): 140 Cs-aspartate, 5 EGTA, 2 $MgCl_2$, 0.1 $CaCl_2$, 2 K_2ATP, and 10 HEPES, pH 7.2 (310 mOsm with sucrose). The external solution for recording Ba^{2+} currents contained the following (in mM): 150 tetraethylammonium Br, 3 KCl, 1.0 $NaHCO_3$, 1.0 $MgCl_2$, 10 HEPES, 4 glucose, and 10 $BaCl_2$, pH 7.4 (320 mOsm with sucrose). Pipettes of resistance 2–4 MΩ were used. An Axopatch 200B amplifier (Molecular Devices) was used, and data were filtered at 1–2 kHz and digitized at 5–10 kHz. Analysis was performed using pClamp7 (Molecular Devices) and Origin 7 (OriginLab Corporation). Current records are shown after leak and residual capacitance current subtraction (P/4 protocol). For determination of the voltage for 50% current activation ($V_{50,act}$), the current density–voltage (*I–V*) relationships were fitted between −30 and +50 mV with a modified Boltzmann equation as follows: $I = G_{max} \times (V - V_{rev})/(1 + \exp(-(V - V_{50,act})/k))$, where I is the current density (in picoamperes per picofarad), G_{max} is the maximum conductance (in nanosiemens per picofarad), V_{rev} is the reversal potential, and k is a slope factor.

Gabapentin binding assay. Binding of [^{3}H]GBP was performed in a final volume of 250 μl at room temperature for 2 h. Cholesterol-rich microdomains (3 μg/tube) were incubated with 10–750 nM [^{3}H]GBP (ARC) in 10 mM HEPES/KOH, pH 7.4, and then rapidly filtered through GF/B filters, presoaked with 0.3% polyethyleneimine. Filters were washed three times with 3 ml of ice-cold 100 mM Tris/HCl, pH 7.4, and the amount of bound [^{3}H]GBP was determined by scintillation counting. Concentrations of [^{3}H]GBP >40 nM were achieved by adding nonradioactive GBP prepared by serial dilutions and correcting the specific binding by the dilution factor, as described previously (Marais et al., 2001). Nonspecific binding was determined in the presence of 1000-fold excess of nonradioactive GBP. Three independent experiments were performed, each in triplicate, and data were analyzed by fitting an equation for a rectangular hyperbola to the specific binding data from each experiment to obtain the dissociation constant (K_D) and maximum number of binding sites (B_{max}). The relationship between the specific binding of GBP (*B*, expressed in picomoles/milligram of protein) and the concentration of free ligand (GBP) present is given by the following equation: $B = (B_{max} \times [GBP])/(K_D + [GBP])$.

αBgTx binding. Cells transfected with bbs-tagged constructs were labeled with 10 μg/ml αBgTx-AF488 (Invitrogen), in HEPES-buffered saline, for 30 min at 17°C. The cells were washed with HBS at 17°C to eliminate any unbound αBgTx and visualized immediately. The cells were imaged using a confocal laser-scanning microscope (Zeiss), using a 63× (NA, 1.2) water-immersion objective. The optical sections were always 1 μm thick.

The quantification of cell surface-expressed $\alpha_2\delta$-2 bbs subunits was determined as described in supplemental Figure S1 (available at www.jneurosci.org as supplemental material). Briefly, a region of interest of constant dimensions was positioned on the membrane of each individual cell, and the fluorescence intensity was measured after subtraction, for each image, of the background corresponding to an area where no cell was present. To observe the internalization of $\alpha_2\delta$-2 bbs, the cells labeled at 17°C were incubated in serum-free growth medium at 37°C, for various times. A region of interest of constant dimensions was positioned across each individual cell, and the corresponding fluorescence intensity profile was plotted and aligned with the image, to define extracellular, membrane, and intracellular areas. The background fluorescence corre-

sponding to the average extracellular signal was subtracted. The evolution over time of the proportion of internal fluorescence above a threshold defined as 40% of the membrane value was measured to assess the rate of endocytosis of the $\alpha_2\delta$-2 bbs subunit. To monitor the insertion of new subunits at the plasma membrane, the cells were preincubated with 10 μg/ml unlabeled αBgTx (Invitrogen) for 30 min at 17°C, and then washed and incubated with 1 μg/ml αBgTx-AF488 for various times at 37°C. The quantification of the fluorescence appearing at the cell surface over time gives an estimation of the rate of insertion of new subunits.

Primary cortical neurons. Primary cortical neurons were obtained from embryonic day 18 Sprague Dawley rat embryos. The cortices were dissected in Hanks buffered salt solution, and the cells were dissociated by trypsinization followed by trituration. The neurons were plated on glass coverslips coated with poly-L-lysine and cultured in Neurobasal medium (Invitrogen) containing B27 supplement (Invitrogen), 100 μg/ml penicillin, 100 μg/ml streptomycin, and 2 mM GlutaMAX (Invitrogen). One-half of the growth medium was replaced every 3 d. After 7–12 d in culture, cortical neurons were transfected using Lipofectamine 2000 (Invitrogen) following the manufacturer's instructions. The cDNA mixes used were enhanced cyan fluorescent protein (eCFP)/$\alpha_2\delta$-2 bbs in a 1:9 ratio and GFP-Rab11/$\alpha_2\delta$-2 bbs in a 2.5:7.5 ratio. The ratio cDNA/Lipofectamine 2000 used was 0.8 μg:4 μl, and after 4 h the medium containing the transfection mix was replaced with a mix of 50% conditioned medium and 50% fresh growth medium. Experiments were performed 72 h after transfection.

Results

Expression of the $\alpha_2\delta$-2 bbs construct

The insertion of a bbs tag in the extracellular loops of membrane proteins has proven useful to assess their cell surface expression and dynamics (Sekine-Aizawa and Huganir, 2004; Wilkins et al., 2008). So far, this method has been used to investigate the trafficking properties of neurotransmitter receptors, tagged at their N terminus. To investigate whether this strategy could be used to study calcium channel subunit trafficking, we engineered an $\alpha_2\delta$-2 subunit with a bbs epitope in its extracellular α_2 region (Fig. 1*A*). In our previous study, an $\alpha_2\delta$-2 subunit engineered with a HA tag introduced in this region was fully functional, and the HA epitope was accessible for antibody binding (Davies et al., 2006).

To test whether αBgTx-Alexa Fluor 488 (AF488) labeled the bbs-tagged $\alpha_2\delta$-2 specifically, we expressed $\alpha_2\delta$-2 bbs, together with $Ca_v2.1$ and the β4 subunit, in tsA-201 cells (Fig. 1*B*). The presence of the tag was detected by incubation with αBgTx-AF488 for 30 min at 17°C; then cells were fixed, and the presence of the $\alpha_2\delta$-2 subunit at the plasma membrane was assessed by immunocytochemistry on nonpermeabilized cells using an antibody directed against an extracellular epitope of $\alpha_2\delta$-2. The cells transfected with untagged subunits (Fig. 1*B*, left) and for which $\alpha_2\delta$-2 immunoreactivity (red, top row) was observed, did not display any significant αBgTx-AF488 fluorescence (green, middle row). Cells transfected with $\alpha_2\delta$-2 bbs (Fig. 1*B*, right) displayed substantial plasma membrane labeling with αBgTx-AF488 and were also labeled by the antibody directed against $\alpha_2\delta$-2. Therefore, αBgTx-AF488 specifically binds to bbs-tagged $\alpha_2\delta$-2.

The functionality of $\alpha_2\delta$-2 bbs was tested in transfected tsA-201 cells, using whole-cell recording (Fig. 1*C*). Calcium channel currents recorded in cells transfected with $Ca_v2.1/\beta4/\alpha_2\delta$-2 were of similar amplitude (peak I_{Ba} at +5 mV was -202.6 ± 59.7 pA/pF; $n = 7$) to those recorded with $Ca_v2.1/\beta4/\alpha_2\delta$-2 bbs, either in the absence (-165.8 ± 39.3 pA/pF; $n = 10$) or in the presence of αBgTx-AF488 (-174.9 ± 39.2 pA/pF; $n = 8$; $p > 0.05$, one-way ANOVA), and the V_{50} for activation were not significantly different between each condition (-2.9 ± 2.2 mV for $Ca_v2.1/\beta4/\alpha_2\delta$-2, compared with -0.5 ± 1.3 mV for $Ca_v2.1/\beta4/\alpha_2\delta$-2 bbs and -1.7 ± 1.5 mV for $Ca_v2.1/\beta4/\alpha_2\delta$-2 bbs in the presence of αBgTx-AF488; $p > 0.05$, one-way ANOVA).

The binding affinity of $\alpha_2\delta$-2 bbs for [^{3}H]GBP was examined in cholesterol-rich microdomains, into which $\alpha_2\delta$-2 subunits were shown to partition (Davies et al., 2006). Both $\alpha_2\delta$-2 and $\alpha_2\delta$-2 bbs displayed a similar affinity for [^{3}H]GBP (Fig. 1*D*) (K_D of 28.5 ± 6.4 and 34.5 ± 6.9 nM, respectively; $n = 3$ experiments; $p > 0.05$, Student's paired t test). This indicates that the bbs epitope does not interfere with the correct folding of $\alpha_2\delta$-2. Moreover, the presence of αBgTx did not affect the total binding of [^{3}H]GBP to $\alpha_2\delta$-2 bbs (supplemental Fig. S2, available at www.jneurosci.org as supplemental material).

Chronic incubation with gabapentin leads to a decrease of $\alpha_2\delta$-2 levels at the plasma membrane

We have previously shown that chronic application of GBP *in vitro* caused a substantial decrease in calcium currents, and this was found to be associated with a reduction in the number of channels present at the plasma membrane (Hendrich et al., 2008). This finding was replicated in the present study using $\alpha_2\delta$-2 bbs (Fig. 2*A*, left column; *B*, top). tsA-201 cells were transfected with $Ca_v2.1/\alpha_2\delta$-2 bbs/β4 and incubated with 100 μM or 1 mM GBP for 48 h, before assessment of the plasma membrane expression level of $\alpha_2\delta$-2 bbs using αBgTx-AF488 labeling as described in supplemental Fig. S1 (available at www.jneurosci.org as supplemental material). Incubation with αBgTx-AF488 was performed at 17°C to reduce any trafficking events and ensure that only plasma membrane $\alpha_2\delta$-2 subunits were labeled. αBgTx-AF488 binding was observed to be stable at 17°C over a 2 h period (supplemental Fig. S1, available at www.jneurosci.org as supplemental material). The level of cell surface fluorescence for $\alpha_2\delta$-2 bbs incubated with 100 μM GBP (Fig. 2*B*, light gray bar) was reduced to 49.3 ± 3.6% of the control value, and to 41.9 ± 3.6% of the control level for cells incubated with 1 mM GBP (Fig. 2*B*, dark gray bar).

It is known that the R282A mutation in $\alpha_2\delta$-2, located within a triple arginine motif known to be crucial for GBP binding to both $\alpha_2\delta$-1 and $\alpha_2\delta$-2, causes a dramatic reduction of affinity for GBP (Wang et al., 1999; Davies et al., 2006). We found that GBP had no significant effect on the surface expression of $\alpha_2\delta$-2 R282A bbs (Fig. 2*A*, right column; *B*, bottom). The level of fluorescence for $\alpha_2\delta$-2 R282A bbs incubated with 100 μM GBP (Fig. 2*B*, light gray bar) corresponded to 96.3 ± 4.7% of the control value, and to 91.6 ± 5.5% of the control after incubation with 1 mM GBP (Fig. 2*A*,*B*). The lack of effect of GBP on the cell surface level of $\alpha_2\delta$-2 R282A bbs confirms that these effects are mediated by the binding of GBP to the $\alpha_2\delta$-2 subunit.

The effect of GBP on the cell surface expression of $\alpha_2\delta$-2 bbs was also examined in primary cultured cortical neurons expressing $\alpha_2\delta$-2 bbs, with free eCFP to visualize the morphology of the transfected cells. Transfected neurons were preincubated with the nicotinic antagonist tubocurarine, which competes with αBgTx for binding to the endogenous α7 nicotinic acetylcholine receptor, without interfering with the binding of αBgTx to the bbs tag (supplemental Fig. S3, available at www.jneurosci.org as supplemental material). Cell surface-expressed $\alpha_2\delta$-2 bbs was then detected by live labeling with αBgTx-AF555, in the presence of tubocurarine. Chronic GBP incubation led to a decrease in the fluorescence in the neurites of the transfected cells (60.7 ± 8.8%

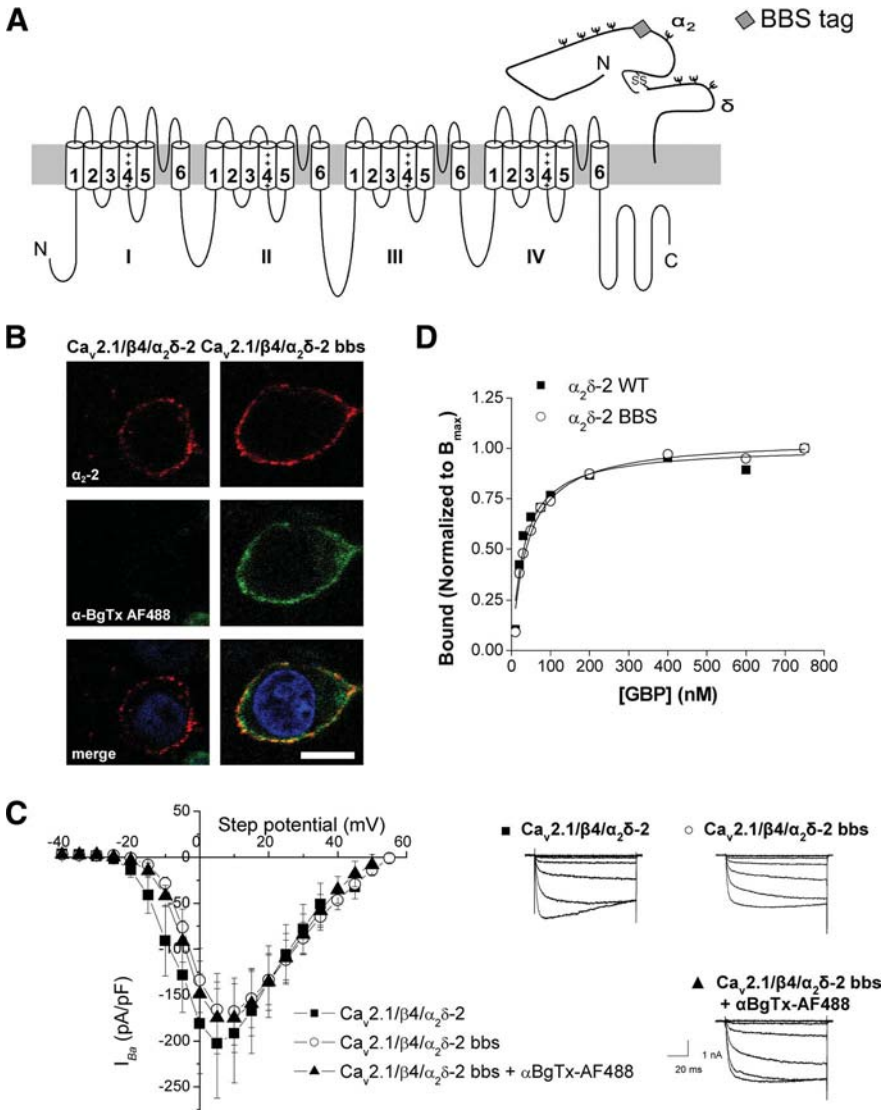

Figure 1. Insertion of a bbs tag in the VGCC $\alpha_2\delta$-2 subunit. ***A***, Schematic representation of a $Ca_v2.1$ and a $\alpha_2\delta$-2 subunit, showing the position of the bbs tag (gray diamond) in $\alpha_2\delta$-2. ***B***, tsA-201 cells were transfected with $Ca_v2.1/\alpha_2\delta$-2/β4 or $Ca_v2.1/\alpha_2\delta$-2 bbs/β4, and labeled with an antibody directed against α_2-2 (102–117 peptide) (red fluorescence; top row) and with αBgTx-AF488 (green; middle row). The merged images also showing nuclear staining with DAPI are shown in the bottom row. The images are 1-μm-thick optical sections. Scale bar, 20 μm. ***C***, *I–V* relationships (left) and representative currents traces resulting from step potentials from −90 mV to between −25 and +5 mV, in 5 mV increments (right) for cells transfected with $Ca_v2.1/\beta4/\alpha_2\delta$-2 (■) ($n = 7$), or $Ca_v2.1/\beta4/\alpha_2\delta$-2 bbs in the absence (○) ($n = 10$) or in the presence of αBgTx-AF488 (▲) ($n = 8$). Error bars indicate SEM. ***D***, Binding isotherm for [^{3}H]GBP to cholesterol-rich microdomains fractions prepared from tsA-201 cells expressing either $\alpha_2\delta$-2 (■) (fitted to an hyperbola with $K_D = 28.5$ nM; $n = 3$) or $\alpha_2\delta$-2 bbs (○) ($K_D = 34.9$ nM; $n = 3$). The binding curves were normalized to each mean B_{max}.

of the fluorescence measured under control conditions) (Fig. 2*C*,*D*).

Gabapentin does not alter the internalization rate of $\alpha_2\delta$-2

We hypothesized that the decrease of plasma membrane levels of $\alpha_2\delta$-2 might be caused by an augmentation of the internalization rate of $\alpha_2\delta$-2, leading to its accumulation in internal compartments or to its degradation. The binding of αBgTx-AF488 to $\alpha_2\delta$-2 bbs or $\alpha_2\delta$-2 R282A bbs was used to monitor the internalization of these proteins. Cells were incubated with αBgTx-AF488 for 30 min at 17°C, so that only cell surface-expressed subunits would be labeled. After washing the unbound αBgTx, cells were returned to 37°C for various times to allow internalization, either in the absence or in the presence of GBP (Fig. 3*A*,*B*). Submembrane punctate fluorescence, likely to correspond to vesicles containing endocytosed $\alpha_2\delta$-2 bbs, rapidly appeared inside the labeled cells (Fig. 3*A*, arrowed), and the amount of internal fluorescence increased concomitantly with a decrease in membrane labeling. The net endocytosis of $\alpha_2\delta$-2 bbs (Fig. 3*A*,*C*) or $\alpha_2\delta$-2 R282A bbs (Fig. 3*B*,*D*) was unaffected by the presence of GBP over a 1 h time period ($p > 0.05$, two-way ANOVA and Bonferroni's post test). However, the proportion of $\alpha_2\delta$-2 R282A bbs that was internalized in 1 h was significantly less than that for the WT $\alpha_2\delta$-2 bbs (Fig. 3*C*,*D*) ($p < 0.05$; $n = 3$ experiments; Student's unpaired *t* test).

To examine whether the fluorescence corresponding to internalized subunits was altered because of quenching or unbinding of αBgTx-AF488 from the bbs tag in the acidified lumen of endosomes, we tested the effect of the application of solutions buffered at pH values in the 4.5–7.4 range on cells expressing $\alpha_2\delta$-2 bbs (supplemental Fig. S4, available at www.jneurosci.org as supplemental material). The cell surface staining by αBgTx-AF488 remained unaltered under all conditions tested.

Gabapentin disrupts the post-Golgi forward trafficking of $\alpha_2\delta$-2

As the endocytosis of $\alpha_2\delta$-2 is not affected by GBP, we used the bbs-tagged $\alpha_2\delta$-2 subunit to assess whether GBP altered the insertion of new $\alpha_2\delta$-2 subunits into the plasma membrane. Cells transfected with $Ca_v2.1/\alpha_2\delta$-2 bbs/β4 were first incubated at 17°C with an excess of unlabeled αBgTx to saturate all cell surface $\alpha_2\delta$-2 subunits. Unlabeled αBgTx efficiently saturated the plasma membrane $\alpha_2\delta$-2 bbs subunits, since no labeling of these cells could be detected after a subsequent incubation with αBgTx-AF488 at 17°C (supplemental Fig. S5, available at www.jneurosci.org as supplemental material). After washing away the unbound αBgTx, the cells were incubated at 37°C with αBgTx-AF488 for various times (Fig. 4*A*). Under these conditions, the αBgTx-AF488 will bind only to $\alpha_2\delta$-2 subunits that are newly inserted into the plasma membrane. When GBP was added to the culture medium for 4 h before the experiment and was present at all times during the assay, this insertion remained unchanged ($p > 0.05$, two-way ANOVA and Bonferroni's post test) (Fig. 4*B*,*C*).

While biosynthesis of new proteins is occurring, the $\alpha_2\delta$-2 subunits inserted at the cell surface will originate both from the pool of newly synthesized proteins and from a pool of preexisting proteins that would be cycling between the plasma membrane and internal compartments (Fig. 4*A*). To determine whether any effect of GBP on the recycling of $\alpha_2\delta$-2 was being masked by the

insertion of newly synthesized proteins, the cells were preincubated with brefeldin A (BFA) (50 ng/ml), which blocks the exit of proteins from the endoplasmic reticulum (ER) and causes disorganization of the Golgi apparatus structure (Lippincott-Schwartz et al., 1989) (Fig. 5*A*). After 5 h of incubation with BFA, the cell surface level of $\alpha_2\delta$-2 bbs was significantly reduced (64.8 ± 4.5% of control values) (supplemental Fig. S6, available at www.jneurosci.org as supplemental material), which indicates that the pool of newly synthesized proteins exiting from the ER has been substantially depleted. After initial BFA application for 4 h, GBP was then applied for an additional 4 h. BFA was present at all times during this assay, as its effects are reversible. Under these conditions, the total amount of $\alpha_2\delta$-2 bbs subunits present at the plasma membrane was not significantly modified by the presence of GBP (data not shown). The insertion of $\alpha_2\delta$-2 bbs into the plasma membrane over 1 h was then assayed according to protocol described in Figure 5*A*. After 30 min incubation at 17°C with αBgTx to mask the $\alpha_2\delta$-2 already present at the plasma membrane, the amount of $\alpha_2\delta$-2 bbs inserted into the plasma membrane over 30 min and 1 h was significantly reduced in the presence of GBP, to 59.4 ± 8.5% of the control value after 1 h ($p < 0.01$, two-way ANOVA and Bonferroni's post test) (Fig. 5*B*,*D*). In contrast, there was no effect of GBP on the insertion of $\alpha_2\delta$-2 R282A bbs (Fig. 5*C*,*E*), and the amount of membrane staining achieved in 1 h for $\alpha_2\delta$-2 R282A bbs was similar to that for $\alpha_2\delta$-2 bbs in the presence of GBP (Fig. 5*C*,*E*). Under the conditions of this experiment, the cells displayed a much reduced fluorescence compared with the experiment performed in the absence of BFA (Fig. 4). This relates to the fact that, in the absence of BFA, most of the newly inserted $\alpha_2\delta$-2 bbs subunits corresponds to newly synthesized proteins, and this might explain the lack of significant effect of GBP in the experiment described in Figure 4. These results indicate that GBP interferes with the forward trafficking of $\alpha_2\delta$-2 bbs after its exit from the Golgi apparatus.

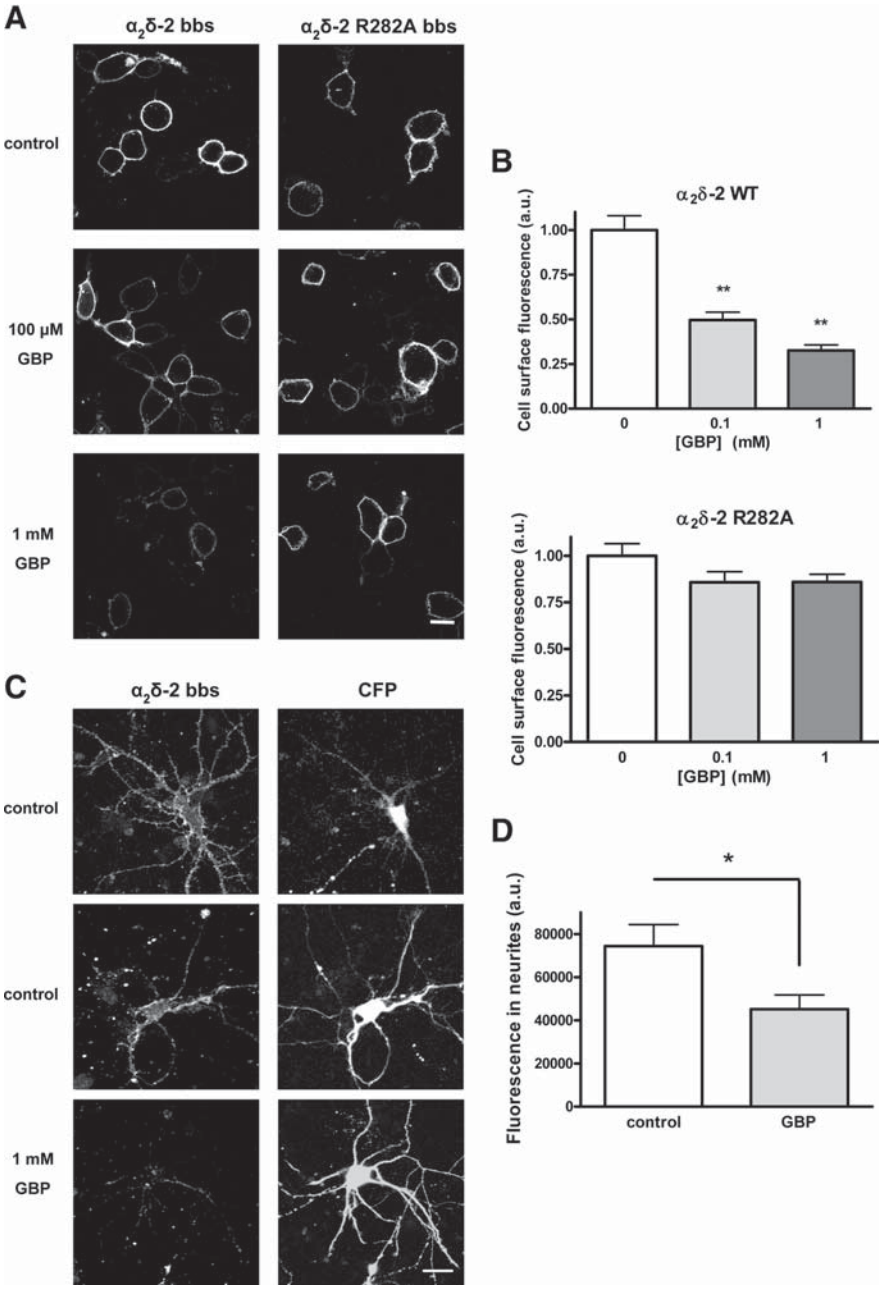

Figure 2. Chronic GBP reduces the cell surface expression of $\alpha_2\delta$-2 bbs. ***A***, tsA-201 cells transfected with $Ca_v2.1/\beta4/\alpha_2\delta$-2 bbs or $Ca_v2.1/\beta4/\alpha_2\delta$-2 R282A bbs were incubated for 40 h with 100 μM or 1 mM GBP, or with addition of the equivalent volume of H_2O (control cells). Plasma membrane-expressed $\alpha_2\delta$-2 bbs was labeled at 17°C with αBgTx-AF488. Scale bar, 10 μm. ***B***, Quantification of the fluorescence at the plasma membrane, measured within a region of interest covering an identical area across the plasma membrane of each cell present in the field of view, for WT $\alpha_2\delta$-2 bbs or for $\alpha_2\delta$-2 R282A bbs for control (white bars), 100 μM GBP (light gray bars), or 1 mM GBP (dark gray bars). The results are expressed as the mean ± SEM from three independent experiments (20–42 cells per condition per experiment). $^{**}p < 0.005$, one way ANOVA and Bonferroni's post test. ***C***, Primary cortical neurons expressing eCFP and $\alpha_2\delta$-2 bbs were incubated for 72 h with 1 mM GBP or the equivalent volume of H_2O (control cells). $\alpha_2\delta$-2 bbs subunits were labeled using αBgTx-AF555, in the presence of 100 μM tubocurarine, to remove any background caused by the binding of αBgTx to α7 nicotinic receptors. All cells analyzed were positive for CFP expression. The panels corresponding to $\alpha_2\delta$-2 bbs labeling correspond to a 1.2-μm-thick optical section, whereas the CFP panels show an average intensity projection of a *z*-stack containing three images. Scale bar, 20 μm. ***D***, Quantification of αBgTx-AF555 labeling of neurites. The fluorescence density was measured in regions of interests corresponding to the neurites of individual neurons, in control condition (white bar) ($n = 19$) or after chronic incubation with GBP (gray bar) ($n = 16$). $^{*}p < 0.05$, Student's unpaired *t* test.

Gabapentin interferes with the Rab11-dependent recycling of $\alpha_2\delta$-2

As our results suggest that GBP does not interfere with the initial trafficking of newly synthesized $\alpha_2\delta$-2, we investigated whether GBP inhibited the trafficking of recycled $\alpha_2\delta$-2. The cycling of membrane proteins between the plasma membrane and endosomal compartments requires various Rab-GTPases, which are involved in the sorting and docking of trafficking vesicles to those compartments (Stenmark, 2009). From the plasma membrane, internalized vesicles are first targeted to early endosomes, from which they can be recycled via a Rab4-dependent pathway, or directed to Rab11-dependent recycling endosomes, or sorted

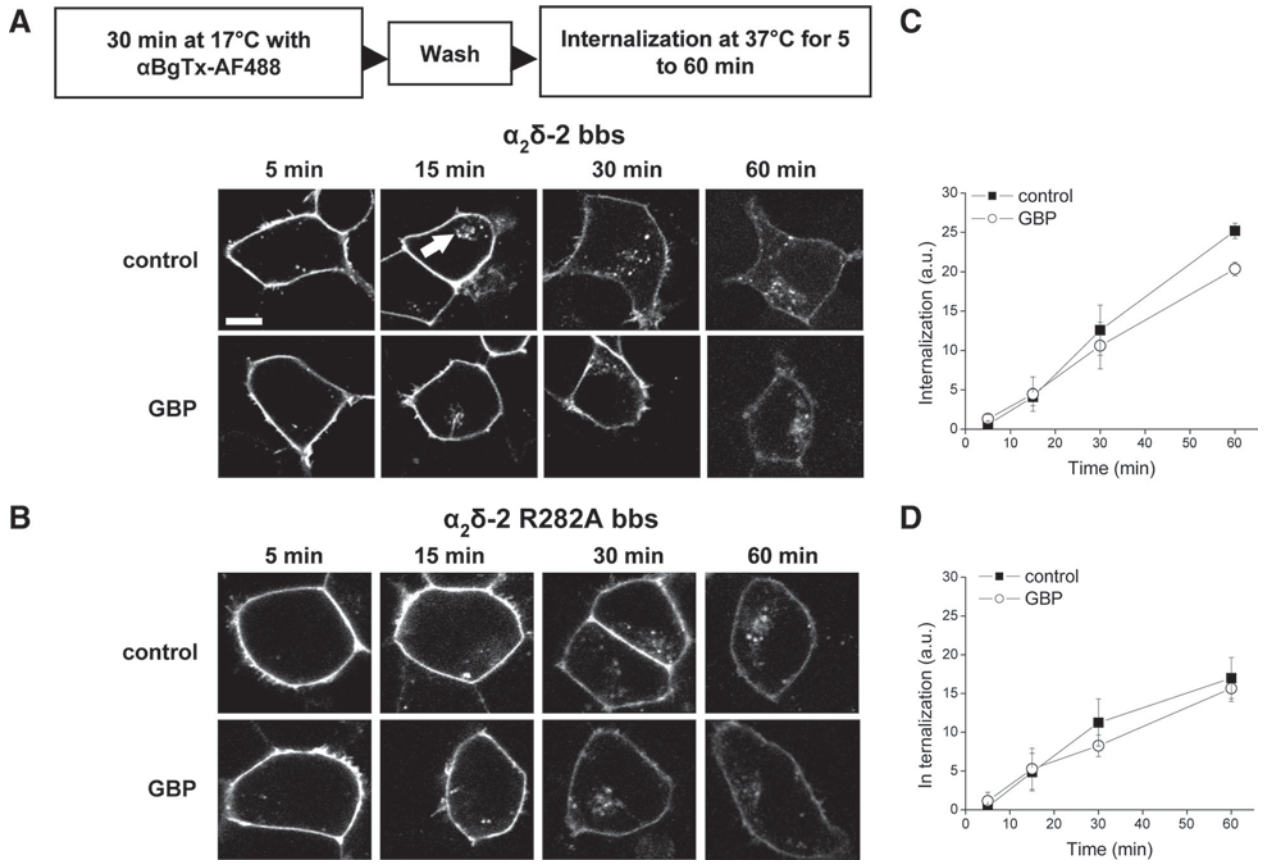

Figure 3. GBP does not affect the internalization rate of $\alpha_2\delta$-2 bbs. ***A***, ***B***, tsA-201 cells transfected with $Ca_v2.1/\beta4/\alpha_2\delta$-2 bbs (***A***) or $Cav2.1/\beta4/\alpha2\delta$-2 R282A bbs (***B***) were incubated with αBgTx-AF488 at 17°C for 30 min, washed to remove free αBgTx-AF488, and then incubated at 37°C to allow internalization of the subunit, in the absence or in the presence of 1 mM GBP, and imaged at the indicated times (5–60 min), as summarized in the protocol above the images. Vesicles containing $\alpha_2\delta$-2 bbs were seen intracellularly (indicated by the white arrow) after incubation at 37°C. Scale bar, 20 μm. ***C***, ***D***, Time course of the internalization of $\alpha_2\delta$-2 bbs (***C***) or $\alpha_2\delta$-2 R282A bbs (***D***), in the presence of 1 mM GBP (○) or control (■). The results are shown as the mean ± SEM of three independent experiments. In each experiment, 16–36 cells were analyzed per time point and condition.

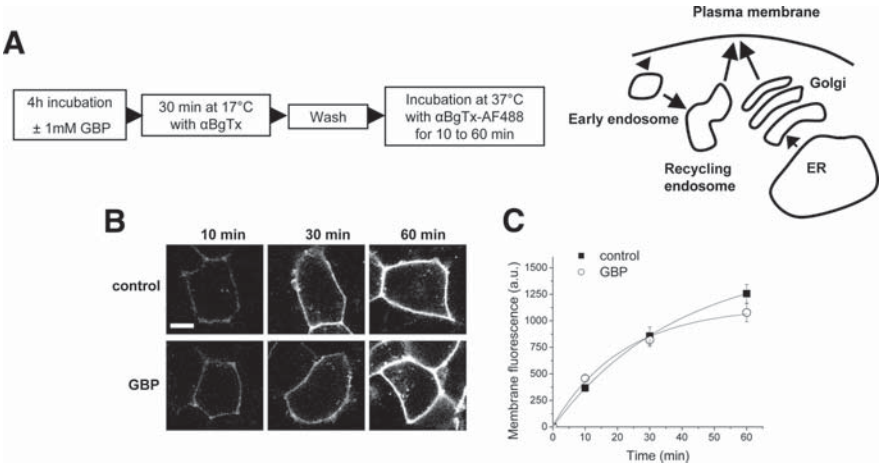

Figure 4. The rate of insertion of $\alpha_2\delta$-2 is not altered after 4 h in the presence of GBP. ***A***, Diagram indicating the possible pathways (right) involved using the insertion assay (left). ***B***, tsA-201 cells expressing $Ca_v2.1/\beta4/\alpha_2\delta$-2 bbs were preincubated for 4 h without (control) or with 1 mM GBP. The cells were then incubated at 17°C with unlabeled αBgTx for 30 min, and then at 37°C with αBgTx-AF488 for the indicated times, as summarized in the protocol in ***A***. Scale bar, 20 μm. ***C***, Quantification of the fluorescence appearing at the plasma membrane over time, in the presence of 1 mM GBP (○) or control (■). The results are expressed as the mean ± SEM of three independent experiments. In each experiment, 14–36 cells were analyzed per time point and condition.

to late endosomes for degradation. Since puncta corresponding to internalized $\alpha_2\delta$-2 bbs were often observed to accumulate in the perinuclear region (Fig. 3*A*, arrowed), we hypothesized that $\alpha_2\delta$-2 bbs might be recycled via the perinuclear Rab11-dependent endocytic recycling compartment (ERC). If this assumption is correct, the coexpression of Rab11 S25N, a dominant-negative mutant of Rab11 that is deficient in GTP binding, will prevent the recycling of $\alpha_2\delta$-2 bbs to the plasma membrane and reduce the steady-state level of cell surface $\alpha_2\delta$-2 bbs (Fig. 6*A*). Our observations were consistent with this hypothesis, as the cell surface level of $\alpha_2\delta$-2 bbs in the presence of Rab11 S25N was significantly reduced compared with expression of WT Rab11 (74.5 ± 3.9% of WT fluorescence levels; two-way ANOVA and Bonferroni's post test, $p < 0.01$) (Fig. 6*B*,*E*).

To determine whether GBP interferes with the recycling of $\alpha_2\delta$-2 bbs, GBP was applied chronically to cells cotransfected with $Ca_v2.1/\beta4/\alpha_2\delta$-2 bbs and Rab11 S25N, and the plasma membrane expression of $\alpha_2\delta$-2 bbs was assayed using αBgTx-AF488 (Fig. 6*B*). In the presence of WT Rab11, chronic GBP produced a significant decrease of the cell surface fluorescence (48.2 ± 2.9% of control), which was comparable with that observed under control conditions (Fig. 6*E*). However, when Rab11 S25N was

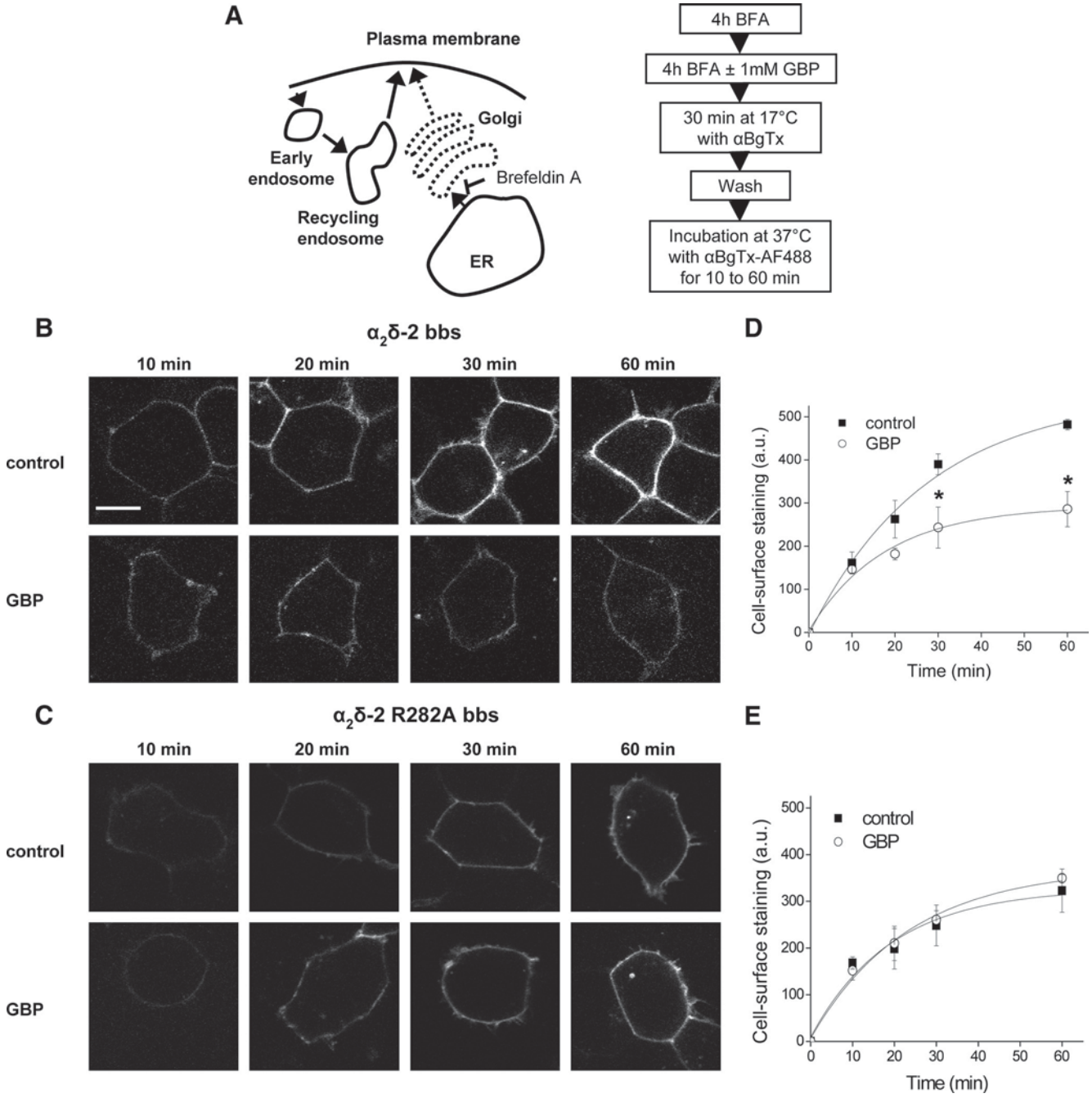

Figure 5. Effect of GBP on the forward trafficking of $\alpha_2\delta$-2 subunits. ***A***, Diagram (left) indicating the possible pathways involved using the assay described (right). ***B***, ***C***, tsA-201 cells expressing $Ca_v2.1/\beta4/\alpha_2\delta$-2 bbs (***B***) or $Ca_v2.1/\beta4/\alpha_2\delta$-2 R282A bbs (***C***) were incubated for 4 h with 50 ng/ml BFA. One millimolar GBP or the equivalent volume of H_2O was subsequently added to the cells for 4 h. The cells were then incubated at 17°C with unlabeled αBgTx for 30 min, and then at 37°C with αBgTx-AF488 for the indicated times, as summarized in the protocol in ***A***. Scale bar, 20 μm. The imaging settings were modified compared with Figure 4 to obtain a better visualization of the cells but were kept constant within the experiment. ***D***, ***E***, Time courses for the insertion of $\alpha_2\delta$-2 bbs (***D***) or $\alpha_2\delta$-2 R282A bbs (***E***) subunits at the plasma membrane, in the presence of 1 mM GBP (○) or control (■). The results are expressed as the mean ± SEM of three independent experiments. In each experiment, 14–41 cells were analyzed per time point and condition. *$p < 0.05$, two-way ANOVA and Bonferroni's post test. The data in ***D*** and ***E*** were fit with single exponentials, to estimate the rate of insertion under the different conditions. The time constant (τ) for the insertion of $\alpha_2\delta$-2 bbs at the plasma membrane was 27.6 min under control conditions and 17.6 min in the presence of GBP (***D***). In contrast, the calculated τ for $\alpha_2\delta$-2 R282A bbs insertion were similar in the absence (19.1 min) and in the presence (23.4 min) of GBP (***E***).

present, GBP did not have any effect on the plasma membrane levels of $\alpha_2\delta$-2 bbs (99.3 ± 5.6% of control).

The effect of GBP on the trafficking of $\alpha_2\delta$-2 through the fast recycling pathway dependent on Rab4-associated endosomes was tested by coexpression of either Rab4 or the dominant-negative GDP-bound Rab4 S22N mutant with $Ca_v2.1/\beta4/\alpha_2\delta$-2 bbs (Fig. 6*C*). The effect of GBP on the cell surface expression of $\alpha_2\delta$-2 bbs under these conditions was examined by labeling with αBgTx-AF488 (Fig. 6*D*). Chronic GBP induced a significant reduction of the cell surface level of $\alpha_2\delta$-2 bbs in the presence of either Rab4 or Rab4 S22N (Fig. 6*F*). Together, these results suggest that GBP exerts its effect on $\alpha_2\delta$-2 by preventing its recycling to the plasma membrane.

To determine whether the effects of Rab11 S25N and GBP on $\alpha_2\delta$-2 trafficking translated to parallel effects on calcium channel currents, we examined the effect of Rab11 S25N on the GBP-

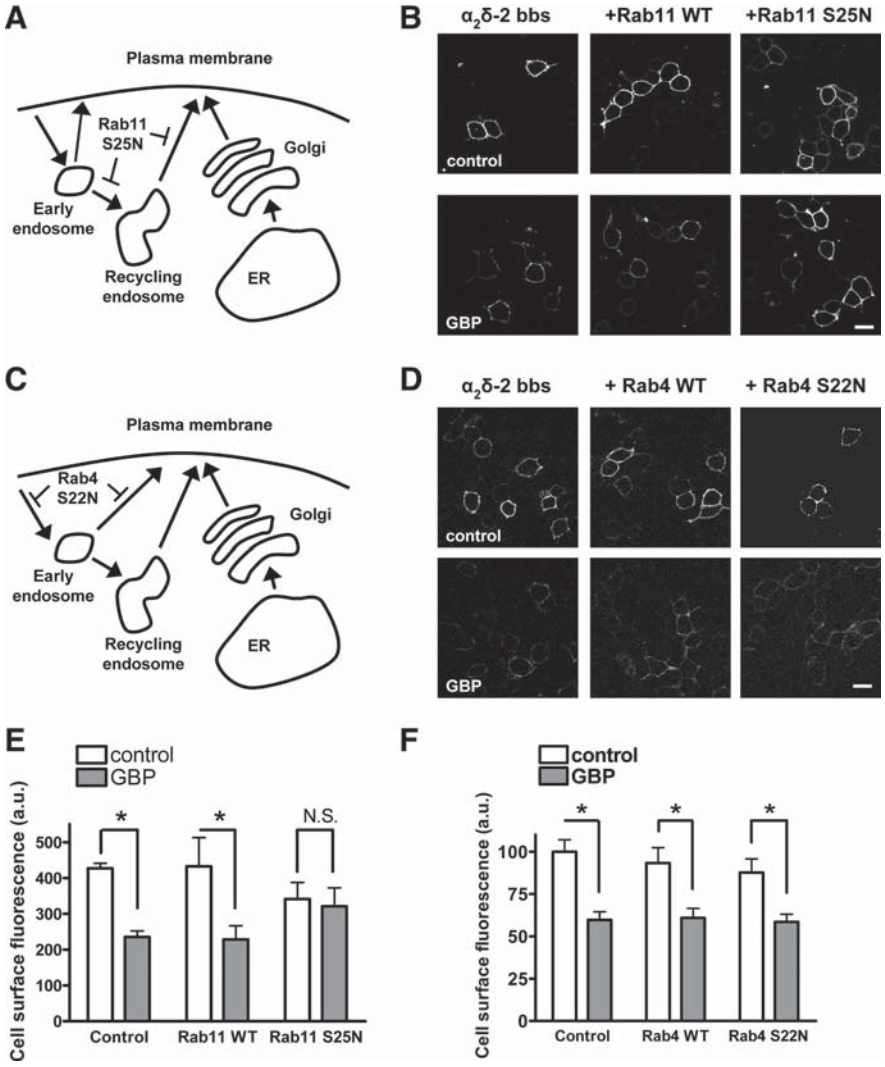

Figure 6. GBP inhibits the trafficking $\alpha_2\delta$-2 through Rab11-associated endosomes. ***A***, Diagram indicating the possible pathways involved using Rab11 S25N. ***B***, Cells transfected with $Ca_v2.1/\beta4/\alpha_2\delta$-2 bbs and either a control cDNA (empty vector), WT Rab11, or Rab11 S25N were incubated with 1 mM GBP for 40 h. The $\alpha_2\delta$-2 subunits present at the plasma membrane were labeled with αBgTx-AF488 at 17°C. Scale bar, 20 μm. ***C***, Diagram indicating the possible pathways involved using Rab4 S22N. ***D***, Cells transfected with $Ca_v2.1/\beta4/\alpha_2\delta$-2 bbs and either a control cDNA (empty vector), WT Rab4, or Rab4 S22N were incubated with 1 mM GBP for 40 h. The $\alpha_2\delta$-2 subunits present at the plasma membrane were labeled with αBgTx-AF555 at 17°C. Scale bar, 20 μm. ***E***, ***F***, Quantification of the fluorescence at the plasma membrane in the absence (white bars) and in the presence of GBP (gray bars) for the three conditions, as indicated, in the presence of Rab11 (***E***) or Rab4 (***F***) constructs. Results are expressed as mean ± SEM of three independent experiments (23–65 cells per condition and per experiment). *$p < 0.05$, two-way ANOVA and Bonferroni's post test.

induced reduction of calcium channel currents in tsA-201 cells (Fig. 7*A*,*B*). Currents recorded from cells expressing $Ca_v2.1/\beta4/\alpha_2\delta$-2, cotransfected with WT Rab11, displayed a 64.7 ± 10.2% reduction when cells were chronically incubated with 1 mM GBP (Fig. 7*C*), in agreement with results obtained previously in the absence of Rab11 (Hendrich et al., 2008). In contrast, when cotransfected with Rab11 S25N, the peak I_{Ba} was reduced compared with that in the presence of WT Rab11, by 50.3 ± 10.6% (two-way ANOVA and Bonferroni's post test, $p < 0.05$), and chronic GBP failed to reduce current amplitude (peak I_{Ba} at +5 mV was −164.9 ± 35.3 mV in the absence, and −172.1 ± 48.7 mV in the presence of chronic GBP) (Fig. 7*C*). These results indicate that the alterations in cell surface levels of $\alpha_2\delta$-2 because of the inhibition of its recycling by GBP induce comparable modification of the number of VGCC complexes at the plasma membrane. Additionally, the peak current amplitude in control cells coexpressing Rab11 S25N is significantly higher than the peak current amplitude from cells expressing Rab11 WT and treated with GBP ($p < 0.05$, two-way ANOVA and Bonferroni's post test).

Effect of GBP on $\alpha_2\delta$-2 expression in neurons

To investigate whether Rab11 S25N would similarly affect the GBP-induced reduction in $\alpha_2\delta$-2 cell surface expression in neurons, we expressed $\alpha_2\delta$-2 with GFP-Rab11 or GFP-Rab11 S25N in primary cortical neurons. The live neurons were first incubated with an antibody directed against the extracellular HA epitope. This method avoids permeabilization of the neurites (supplemental Fig. S7, available at www.jneurosci.org as supplemental material) and thus allows the specific detection of the $\alpha_2\delta$-2 subunits expressed at the plasma membrane (Glynn and McAllister, 2006; Watschinger et al., 2008). After fixation, the neurons were permeabilized and incubated with antibodies against GFP, to strengthen the detection of Rab11, and MAP2, to visualize the morphology of the cells. When GFP-Rab11 WT was expressed, chronic GBP induced a significant decrease in cell surface labeling of $\alpha_2\delta$-2 surface fluorescence in the neurites to 59.9 ± 4.4% of the control value (Fig. 8*B*,*C*). However, in the presence of GFP-Rab11 S25N, the $\alpha_2\delta$-2 cell surface fluorescence was not significantly modified by the addition of GBP (105.4 ± 10.7% of control). This indicates that GBP also disrupts the Rab11-dependent recycling of $\alpha_2\delta$-2 in neurons.

Discussion

Gabapentinoid drugs exert their therapeutic effect via binding to the $\alpha_2\delta$-1 and -2 subunits of VGCCs (Davies et al., 2007). Although we have previously shown that GBP disrupts the cell surface expression of VGCCs (Heblich et al., 2008; Hendrich et al., 2008), its mechanism of action remained unclear. Here, we demonstrate that GBP acts intracellularly to prevent the recycling of $\alpha_2\delta$-2 to the plasma membrane from Rab11-associated endosomes, causing a reduction of the number of VGCC complexes at the plasma membrane.

The trafficking properties of $\alpha_2\delta$ subunits are closely linked to their role as a target of gabapentinoid drugs. We previously reported that, *in vitro*, chronic application of GBP induces a substantial diminution of calcium currents, by reducing the number of $\alpha_2\delta$ and $Ca_v\alpha_1$ subunits at the plasma membrane (Hendrich et al., 2008). This mechanism may also be responsible for the role of gabapentinoid drugs in alleviating neuropathic pain after nerve injury, when $\alpha_2\delta$-1 is upregulated in the spinal cord (Newton et al., 2001; Li et al., 2004). This increase in $\alpha_2\delta$-1 is crucial for the establishment of neuropathic pain (Li et al., 2006), and the bind-

ing of PGB or GBP to $\alpha_2\delta$-1 is essential for their therapeutic effect (Field et al., 2006). We have recently found that concomitantly with its effect in alleviating neuropathic pain, PGB disrupts the trafficking of $\alpha_2\delta$-1 to presynaptic terminals (Bauer et al., 2009). In that study, we hypothesized that this would reduce the consequent increase in neurotransmitter release and spinal sensitization associated with neuropathic pain.

In the present study, we have used a bbs-tagged version of $\alpha_2\delta$-2 to examine the trafficking of $\alpha_2\delta$-2 to and from the plasma membrane, and the modulation of these processes by GBP. Our electrophysiological results demonstrated that the $\alpha_2\delta$-2 bbs subunit displays electrophysiological properties comparable with the WT $\alpha_2\delta$-2, even when bound to αBgTx. Therefore, it is highly suitable for monitoring the dynamics of $\alpha_2\delta$-2 at the surface of cells. This method demonstrates that, within minutes, $\alpha_2\delta$-2 subunits undergo constitutive endocytosis and are reinserted to the plasma membrane from intracellular compartments. This dynamic trafficking of $\alpha_2\delta$-2 might be related to the localization of $\alpha_2\delta$-2 subunits in lipid microdomains, which are known to contain constituents of the endocytotic/exocytotic machinery (Davies et al., 2006), and to our finding that $\alpha_2\delta$ subunits form glycosylphosphatidylinositol (GPI)-anchored proteins (Davies et al., 2010), since GPI-anchored proteins undergo endocytosis via specific pathways (Lakhan et al., 2009). Furthermore, the lipid raft localization of the $\alpha_2\delta$-2 proteins might be disrupted depending on the physiological or pathological state of the cells (Davies et al., 2006).

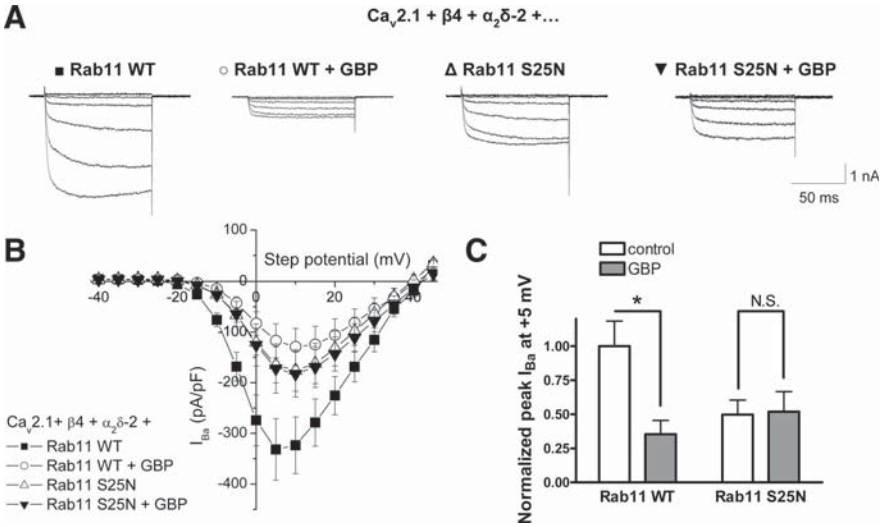

Figure 7. The Rab11 pathway is involved in the reduction of calcium currents by chronic GBP. ***A***, Representative currents traces resulting from step potentials from −90 mV to between −25 mV and +5 mV, in 5 mV increments for cells transfected with $Ca_v2.1/\beta4/\alpha_2\delta$-2/WT Rab11 in the absence (■) or the presence of chronic GBP (○), or $Ca_v2.1/\beta4/\alpha_2\delta$-2/Rab11 S25N in the absence (△) or in the presence of chronic GBP (▼). ***B***, *I–V* relationships for cells transfected with $Ca_v2.1/\beta4/\alpha_2\delta$-2/WT Rab11 under control conditions (■) ($n = 13$) or after chronic incubation with 1 mM GBP (○) ($n = 10$), or $Ca_v2.1/\beta4/\alpha_2\delta$-2/Rab11 S25N in the absence (△) ($n = 13$) or in the presence (▼) ($n = 12$) of chronic GBP. ***C***, Mean peak I_{Ba} calculated at +5 mV and normalized to the value of the control condition, in the absence (white bars) and in the presence (gray bars) of GBP. $^*p < 0.05$, two-way ANOVA and Bonferroni's post test.

Using $\alpha_2\delta$-2 bbs, we have also provided direct evidence that GBP does not modify the endocytic rate of $\alpha_2\delta$-2, but instead it slows the insertion of $\alpha_2\delta$-2 subunits into the plasma membrane. These results are in accordance with the previous observation that chronic GBP acts intracellularly to disrupt the trafficking of $\alpha_2\delta$-2 (Hendrich et al., 2008). We can also conclude that GBP does not block the exit of newly synthesized proteins from the ER to the Golgi apparatus, as such an effect would be masked by the Golgi-disrupting drug BFA. Furthermore, the dominant-negative Rab11 S25N, but not the dominant-negative Rab4 S22N, prevents GBP-induced suppression of $\alpha_2\delta$-2 trafficking. This indicates that GBP interferes with the recycling of internalized subunits between the ERC and the cell surface, but does not interfere with their fast recycling through Rab4-associated endosomes. The fact that cell surface expression of $\alpha_2\delta$-2 coexpressed with Rab11 S25N was significantly higher, rather than lower, than the suppression achieved by GBP when WT Rab11 or no exogenous Rab11 was expressed, suggests that the absence of effect of GBP is not attributable to the fact that $\alpha_2\delta$-2 has already been maximally depleted from the plasma membrane.

It is notable that the recycling through the Rab11 pathway is an important mechanism by which the steady-state cell surface levels of other ion channels is regulated, such as $K_v1.5$ channels (Balse et al., 2009), KCNQ1/KCNE1channels (Seebohm et al., 2007), or epithelial TRPV5 and TRPV6 channels (van de Graaf et al., 2006). Our observation that coexpression of Rab11 S25N leads to reduced levels of $\alpha_2\delta$-2 at the plasma membrane indicates that this pathway is also a major recycling route for $\alpha_2\delta$-2.

The expression of Rab11 S25N in primary neurons also prevented the GBP-induced reduction of plasma membrane-expressed $\alpha_2\delta$-2 in neurites. Therefore, the GBP-mediated reduction in forward trafficking of $\alpha_2\delta$ observed in neurons is also attributable to an inhibition of its Rab11-dependent recycling. Rab11 has been identified in many neuronal types as mainly residing in the somatodendritic compartment (Sheehan et al., 1996; Ng and Tang, 2008), but it is also a constituent of synaptic vesicles (Takamori et al., 2006). The Rab11-dependent recycling of $\alpha_2\delta$-2 in neurons might thus relate both to the regulation of the plasma membrane levels of VGCCs in dendrites and at presynaptic terminals.

This mechanism of action of gabapentinoid drugs provides an explanation for the fact that many studies reported little or no acute effects of GBP on calcium currents or neurotransmitter release (Martin et al., 2002; Fehrenbacher et al., 2003; Brown and Randall, 2005). For GBP to produce a noticeable effect would require that a significant fraction of the plasma membrane pool of $\alpha_2\delta$ subunits had already undergone endocytosis, as was observed in our experiments. Also, it is likely that the rate of cycling of $\alpha_2\delta$ subunits is variable in different cell types, at different locations within the cell, and depending on the physiological state of the cell. For instance, it has been reported that GBP acutely reduced glutamate release in trigeminal neurons only after activation by protein kinase C (Maneuf and McKnight, 2001). Interestingly, protein kinase C activation has been shown to lead to an increased insertion of calcium channels of the Ca_v2 family at the plasma membrane (Zhang et al., 2008). This also reflects previous experimental findings that the observation of effects of GBP *in vitro* depends on culture conditions (Alden and García, 2001; Martin et al., 2002).

Although it has been hypothesized that GBP acts by disrupting the interaction between $\alpha_2\delta$ and α_1 subunits, a previous study

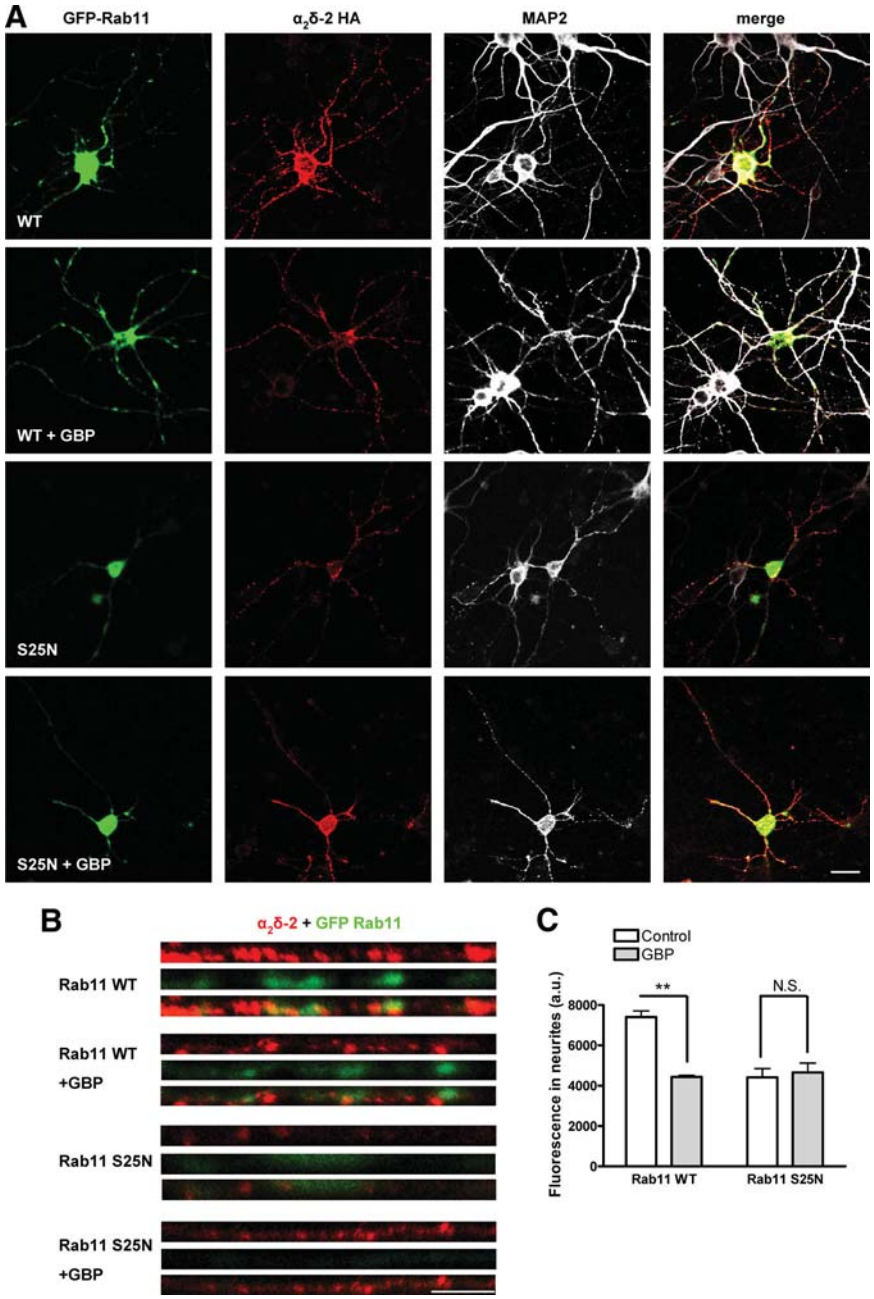

Figure 8. Effect of GBP and Rab11 S25N on $\alpha_2\delta$-2 expression in primary cortical neurons. ***A***, Cortical neurons were cultured for 5–6 d, and then transfected with $\alpha_2\delta$-2 HA and either GFP-Rab11 WT or GFP-Rab11 S25N, and incubated for 3 d in the absence or in the presence of 1 mM GBP for 72 h. Cell surface $\alpha_2\delta$-2 was detected by live labeling using an antibody directed against the HA epitope (column 2) before fixation and permeabilization of the cells and immunodetection of GFP-Rab11 constructs using an antibody directed against GFP (column 1), and MAP2, detected using a Cy5-conjugated secondary antibody (column 3). A merged imaged is shown in column 4. GFP-Rab11 S25N displays a diffuse localization corresponding to its lack of association with cellular membranes. Scale bar, 20 μm. ***B***, Enlarged images of straightened neurite segments, localized 200–300 μm from the cell body, stained for cell surface-expressed $\alpha_2\delta$-2 (red) and for GFP-Rab11 (green). Scale bar, 5 μm. ***C***, Quantification of the fluorescence density corresponding to the cell surface immunoreactivity for $\alpha_2\delta$-2 in neurites segments, in the absence (white bars) or in the presence (gray bar) of 1 mM GBP. The results are expressed as the mean ± SEM of 11–22 cells from four independent experiments. $^{**}p < 0.001$, two-way ANOVA and Bonferroni's post test.

observed that the VGCC complex remained intact in the presence of GBP (Kang et al., 2002). According to our results, GBP only prevents the correct trafficking of $\alpha_2\delta$, which in turn affects the trafficking of α_1 subunits. Therefore, the study of the trafficking of $\alpha_2\delta$ reflects the trafficking of α_1 subunits, consistent with previous observations (Canti et al., 2005). Future work will examine whether $\alpha_2\delta$ subunits are involved in shuttling α_1 subunits to the cell surface, or whether they always remain in subsequent association with α_1 subunits at the plasma membrane.

A recent study showed that $\alpha_2\delta$-1 interacts with thrombospondins (TSPs) and that this binding is essential for the synaptogenic activity of TSPs (Eroglu et al., 2009). According to this study, GBP prevented the interaction of $\alpha_2\delta$-1 with TSPs, thus reducing the TSP-mediated synaptogenesis. It is possible that GBP also prevents the interaction between $\alpha_2\delta$ and TSP at an intracellular location, especially since TSP1 is known to be rapidly internalized (Godyna et al., 1995), and TSP4 is upregulated together with $\alpha_2\delta$-1 in DRGs in experimental neuropathic pain (Wang et al., 2002). Furthermore, it is of interest that GBP was only found to prevent synapse formation when applied during synaptogenesis but did not disrupt established synapses (Eroglu et al., 2009).

GBP only binds to the $\alpha_2\delta$-1 and $\alpha_2\delta$-2 subunits that contain a von Willebrand factor A (VWA) domain with a perfect metal ion adhesion site (MIDAS) motif (Whittaker and Hynes, 2002; Canti et al., 2005; Davies et al., 2007). This domain is also found in integrins, where it mediates conformational changes on binding of a divalent ion to the MIDAS motif (Springer, 2006). In $\alpha_2\delta$ subunits, an intact VWA domain is required for their trafficking to the plasma membrane (Canti et al., 2005). The RRR motif, involved in GBP binding to $\alpha_2\delta$-1 and $\alpha_2\delta$-2, is situated just before the VWA domain. Previously, we hypothesized that GBP binds to $\alpha_2\delta$-2 and displaces an endogenous ligand important for the correct functioning of $\alpha_2\delta$-2 (Davies et al., 2006; Field et al., 2006). Consistent with this hypothesis is the fact that $\alpha_2\delta$-2 R282A and the equivalent $\alpha_2\delta$-1 R217A mutant do not enhance calcium currents to the same extent as their WT counterparts (Davies et al., 2006; Field et al., 2006; Hendrich et al., 2008), which we attributed to a reduced trafficking of these mutants. In this study, we confirmed that $\alpha_2\delta$-2 R282A is internalized and inserted in the plasma membrane to a reduced extent compared with WT $\alpha_2\delta$-2. This result supports the idea that the binding of $\alpha_2\delta$-2 to this endogenous ligand could induce conformational changes that mediate its association with a protein involved in the correct sorting of $\alpha_2\delta$-2 to recycling endosomes. Future work will assess the nature of the endogenous ligand(s) of $\alpha_2\delta$-2 and how they regulate the normal trafficking of these subunits.

References

Alden KJ, García J (2001) Differential effect of gabapentin on neuronal and muscle calcium currents. J Pharmacol Exp Ther 297:727–735.

Arikkath J, Campbell KP (2003) Auxiliary subunits: essential components of the voltage-gated calcium channel complex. Curr Opin Neurobiol 13:298–307.

Balse E, El-Haou S, Dillanian G, Dauphin A, Eldstrom J, Fedida D, Coulombe A, Hatem SN (2009) Cholesterol modulates the recruitment of Kv1.5 channels from Rab11-associated recycling endosome in native atrial myocytes. Proc Natl Acad Sci U S A 106:14681–14686.

Barclay J, Balaguero N, Mione M, Ackerman SL, Letts VA, Brodbeck J, Canti C, Meir A, Page KM, Kusumi K, Perez-Reyes E, Lander ES, Frankel WN, Gardiner RM, Dolphin AC, Rees M (2001) Ducky mouse phenotype of epilepsy and ataxia is associated with mutations in the *Cacna2d2* gene and decreased calcium channel current in cerebellar Purkinje cells. J Neurosci 21:6095–6104.

Bauer CS, Nieto-Rostro M, Rahman W, Tran-Van-Minh A, Ferron L, Douglas L, Kadurin I, Sri Ranjan Y, Fernandez-Alacid L, Millar NS, Dickenson AH, Lujan R, Dolphin AC (2009) The increased trafficking of the calcium channel $\alpha2\delta$-1 to presynaptic terminals in neuropathic pain is inhibited by the $\alpha2\delta$ ligand pregabalin. J Neurosci 29:4076–4088.

Bernstein GM, Jones OT (2007) Kinetics of internalization and degradation of N-type voltage-gated calcium channels: role of the $\alpha_2\delta$ subunit. Cell Calcium 41:27–40.

Brickley K, Campbell V, Berrow N, Leach R, Norman RI, Wray D, Dolphin AC, Baldwin SA (1995) Use of site-directed antibodies to probe the topography of the α_2 subunit of voltage-gated Ca^{2+} channels. FEBS Lett 364:129–133.

Brodbeck J, Davies A, Courtney MJ, Meir A, Balaguero N, Canti C, Moss FJ, Page KM, Pratt WS, Hunt SP, Barclay J, Rees M, Dolphin AC (2002) The ducky mutation in *Cacna2d2* results in altered Purkinje cell morphology and is associated with the expression of a truncated $\alpha_2\delta$-2 protein with abnormal function. J Biol Chem 277:7684–7693.

Brown JP, Dissanayake VU, Briggs AR, Milic MR, Gee NS (1998) Isolation of the [^{3}H]gabapentin-binding protein/$\alpha_2\delta$ Ca^{2+} channel subunit from porcine brain: development of a radioligand binding assay for $\alpha_2\delta$ subunits using [^{3}H]leucine. Anal Biochem 255:236–243.

Brown JT, Randall A (2005) Gabapentin fails to alter P/Q-type Ca^{2+} channel-mediated synaptic transmission in the hippocampus in vitro. Synapse 55:262–269.

Canti C, Nieto-Rostro M, Foucault I, Heblich F, Wratten J, Richards MW, Hendrich J, Douglas L, Page KM, Davies A, Dolphin AC (2005) The metal-ion-dependent adhesion site in the von Willebrand factor-A domain of $\alpha_2\delta$ subunits is key to trafficking voltage-gated Ca^{2+} channels. Proc Natl Acad Sci U S A 102:11230–11235.

Catterall WA (2000) Structure and regulation of voltage-gated Ca^{2+} channels. Annu Rev Cell Dev Biol 16:521–555.

Cheng JK, Lee SZ, Yang JR, Wang CH, Liao YY, Chen CC, Chiou LC (2004) Does gabapentin act as an agonist at native $GABA_B$ receptors? J Biomed Sci 11:346–355.

Cooper ST, Millar NS (1998) Host cell-specific folding of the neuronal nicotinic receptor alpha8 subunit. J Neurochem 70:2585–2593.

Davies A, Douglas L, Hendrich J, Wratten J, Tran-Van-Minh A, Foucault I, Koch D, Pratt WS, Saibil HR, Dolphin AC (2006) The calcium channel $\alpha_2\delta$-2 subunit partitions with $Ca_V2.1$ into lipid rafts in cerebellum: implications for localization and function. J Neurosci 26:8748–8757.

Davies A, Hendrich J, Tran-Van-Minh A, Wratten J, Douglas L, Dolphin AC (2007) Functional biology of the alpha(2)delta subunits of voltage-gated calcium channels. Trends Pharmacol Sci 28:220–228.

Davies A, Kadurin I, Alvarez-Laviada A, Douglas L, Bauer CS, Nieto-Rostro M, Pratt WS, Dolphin AC (2010) The $\alpha2\delta$ subunits of voltage-gated calcium channels form GPI-anchored proteins, a post-translational modification essential for function. Proc Natl Acad Sci U S A 107:1654–1659.

Dupré DJ, Robitaille M, Ethier N, Villeneuve LR, Mamarbachi AM, Hébert TE (2006) Seven transmembrane receptor core signaling complexes are assembled prior to plasma membrane trafficking. J Biol Chem 281:34561–34573.

Eroglu C, Allen NJ, Susman MW, O'Rourke NA, Park CY, Ozkan E, Chakraborty C, Mulinyawe SB, Annis DS, Huberman AD, Green EM, Lawler J, Dolmetsch R, Garcia KC, Smith SJ, Luo ZD, Rosenthal A, Mosher DF, Barres BA (2009) Gabapentin receptor $\alpha_2\delta$-1 is a neuronal thrombospondin receptor responsible for excitatory CNS synaptogenesis. Cell 139:1–13.

Fehrenbacher JC, Taylor CP, Vasko MR (2003) Pregabalin and gabapentin reduce release of substance P and CGRP rat spinal tissues only after inflammation or activation of protein kinase C. Pain 105:133–141.

Field MJ, Cox PJ, Stott E, Melrose H, Offord J, Su TZ, Bramwell S, Corradini L, England S, Winks J, Kinloch RA, Hendrich J, Dolphin AC, Webb T, Williams D (2006) Identification of the $\alpha_2\delta_1$ subunit of voltage-dependent calcium channels as a molecular target for pain mediating the analgesic actions of pregabalin. Proc Natl Acad Sci U S A 103:17537–17542.

Glynn MW, McAllister AK (2006) Immunocytochemistry and quantification of protein colocalization in cultured neurons. Nat Protoc 1:1287–1296.

Godyna S, Liau G, Popa I, Stefansson S, Argraves WS (1995) Identification of the low density lipoprotein receptor-related protein (LRP) as an endocytic receptor for thrombospondin-1. J Cell Biol 129:1403–1410.

Heblich F, Tran Van Minh A, Hendrich J, Watschinger K, Dolphin AC (2008) Time course and specificity of the pharmacological disruption of the trafficking of voltage-gated calcium channels by gabapentin. Channels 2:4–9.

Hendrich J, Tran-Van-Minh A, Nieto-Rostro M, Heblich F, Watschinger K, Striessnig J, Wratten J, Davies A, Dolphin AC (2008) Pharmacological disruption of calcium channel trafficking by the $\alpha_2\delta$ ligand gabapentin. Proc Natl Acad Sci U S A 105:3628–3633.

Ivanov SV, Ward JM, Tessarollo L, McAreavey D, Sachdev V, Fananapazir L, Banks MK, Morris N, Djurickovic D, Devor-Henneman DE, Wei MH, Alvord GW, Gao B, Richardson JA, Minna JD, Rogawski MA, Lerman MI (2004) Cerebellar ataxia, seizures, premature death, and cardiac abnormalities in mice with targeted disruption of the *Cacna2d2* gene. Am J Pathol 165:1007–1018.

Jensen AA, Mosbacher J, Lingenhoehl K, Lohmann T, Johansen TN, Abrahamsen B, Mattsson JP, Lehmann A, Bettler B, Bräuner-Osborne H (2002) The anticonvulsant gabapentin (Neurontin) does not act through gamma-aminobutyric acid-B receptors. Mol Pharmacol 61:1377–1384.

Kang MG, Felix R, Campbell KP (2002) Long-term regulation of voltage-gated Ca^{2+} channels by gabapentin. FEBS Lett 528:177–182.

Klugbauer N, Lacinová L, Marais E, Hobom M, Hofmann F (1999) Molecular diversity of the calcium channel $\alpha_2\delta$ subunit. J Neurosci 19:684–691.

Kocsis E, Trus BL, Steer CJ, Bisher ME, Steven AC (1991) Image averaging of flexible fibrous macromolecules: the clathrin triskelion has an elastic proximal segment. J Struct Biol 107:6–14.

Lakhan SE, Sabharanjak S, De A (2009) Endocytosis of glycosylphosphatidylinositol-anchored proteins. J Biomed Sci 16:93.

Lanneau C, Green A, Hirst WD, Wise A, Brown JT, Donnier E, Charles KJ, Wood M, Davies CH, Pangalos MN (2001) Gabapentin is not a GABAB receptor agonist. Neuropharmacology 41:965–975.

Li CY, Song YH, Higuera ES, Luo ZD (2004) Spinal dorsal horn calcium channel $\alpha_2\delta$-1 subunit upregulation contributes to peripheral nerve injury-induced tactile allodynia. J Neurosci 24:8494–8499.

Li CY, Zhang XL, Matthews EA, Li KW, Kurwa A, Boroujerdi A, Gross J, Gold MS, Dickenson AH, Feng G, Luo ZD (2006) Calcium channel alpha(2)delta(1) subunit mediates spinal hyperexcitability in pain modulation. Pain 125:20–34.

Lippincott-Schwartz J, Yuan LC, Bonifacino JS, Klausner RD (1989) Rapid redistribution of Golgi proteins into the ER in cells treated with brefeldin A: evidence for membrane cycling from Golgi to ER. Cell 56:801–813.

Maneuf YP, McKnight AT (2001) Block by gabapentin of the facilitation of glutamate release from rat trigeminal nucleus following activation of protein kinase C or adenylyl cyclase. Br J Pharmacol 134:237–240.

Marais E, Klugbauer N, Hofmann F (2001) Calcium channel $\alpha_2\delta$ subunits—structure and gabapentin binding. Mol Pharm 59:1243–1248.

Martin DJ, McClelland D, Herd MB, Sutton KG, Hall MD, Lee K, Pinnock RD, Scott RH (2002) Gabapentin-mediated inhibition of voltage-activated Ca^{2+} channel currents in cultured sensory neurones is dependent on culture conditions and channel subunit expression. Neuropharmacology 42:353–366.

McCaffrey MW, Bielli A, Cantalupo G, Mora S, Roberti V, Santillo M, Drummond F, Bucci C (2001) Rab4 affects both recycling and degradative endosomal trafficking. FEBS Lett 495:21–30.

Newton RA, Bingham S, Case PC, Sanger GJ, Lawson SN (2001) Dorsal root ganglion neurons show increased expression of the calcium channel

$\alpha_2\delta$-1 subunit following partial sciatic nerve injury. Brain Res Mol Brain Res 95:1–8.

Ng EL, Tang BL (2008) Rab GTPases and their roles in brain neurons and glia. Brain Res Rev 58:236–246.

Seebohm G, Strutz-Seebohm N, Birkin R, Dell G, Bucci C, Spinosa MR, Baltaev R, Mack AF, Korniychuk G, Choudhury A, Marks D, Pagano RE, Attali B, Pfeufer A, Kass RS, Sanguinetti MC, Tavare JM, Lang F (2007) Regulation of endocytic recycling of KCNQ1/KCNE1 potassium channels. Circ Res 100:686–692.

Sekine-Aizawa Y, Huganir RL (2004) Imaging of receptor trafficking by using α-bungarotoxin-binding-site-tagged receptors. Proc Natl Acad Sci U S A 101:17114–17119.

Sheehan D, Ray GS, Calhoun BC, Goldenring JR (1996) A somatodendritic distribution of Rab11in rabbit brain neurons. Neuroreport 7:1297–1300.

Springer TA (2006) Complement and the multifaceted functions of VWA and integrin I domains. Structure 14:1611–1616.

Stenmark H (2009) Rab GTPases as coordinators of vesicle traffic. Nat Rev Mol Cell Biol 10:513–525.

Sutton KG, Martin DJ, Pinnock RD, Lee K, Scott RH (2002) Gabapentin inhibits high-threshold calcium channel currents in cultures rat dorsal root ganglion neurones. Br J Pharmacol 135:257–265.

Takamori S, Holt M, Stenius K, Lemke EA, Grønborg M, Riedel D, Urlaub H, Schenck S, Brügger B, Ringler P, Müller SA, Rammner B, Gräter F, Hub JS, De Groot BL, Mieskes G, Moriyama Y, Klingauf J, Grubmüller H, Heuser J, et al. (2006) Molecular anatomy of a trafficking organelle. Cell 127:831–846.

van de Graaf SF, Chang Q, Mensenkamp AR, Hoenderop JG, Bindels RJ (2006) Direct interaction with Rab11a targets the epithelial Ca^{2+} channels TRPV5 and TRPV6 to the plasma membrane. Mol Cell Biol 26:303–312.

Wang H, Sun H, Della Penna K, Benz RJ, Xu J, Gerhold DL, Holder DJ, Koblan KS (2002) Chronic neuropathic pain is accompanied by global changes in gene expression and shares pathobiology with neurodegenerative diseases. Neuroscience 114:529–546.

Wang M, Offord J, Oxender DL, Su TZ (1999) Structural requirement of the calcium-channel subunit $\alpha_2\delta$ for gabapentin binding. Biochem J 342:313–320.

Watschinger K, Horak SB, Schulze K, Obermair GJ, Wild C, Koschak A, Sinnegger-Brauns MJ, Tampé R, Striessnig J (2008) Functional properties and modulation of extracellular epitope-tagged $Ca_v2.1$ voltage-gated calcium channels. Channels 2:461–473.

Whittaker CA, Hynes RO (2002) Distribution and evolution of von Willebrand/integrin A domains: widely dispersed domains with roles in cell adhesion and elsewhere. Mol Biol Cell 13:3369–3387.

Wilkins ME, Li X, Smart TG (2008) Tracking cell-surface $GABA_B$ receptors using an α-bungarotoxin tag. J Biol Chem 283:34745–34752.

Zhang Y, Helm JS, Senatore A, Spafford JD, Kaczmarek LK, Jonas EA (2008) PKC-induced intracellular trafficking of Ca_v2 precedes its rapid recruitment to the plasma membrane. J Neurosci 28:2601–2612.